Landau–de Gennes theory of the chevron structure in a smectic-A liquid crystal

S. Kralj* and T. J. Sluckin
Department of Mathematics, University of Southampton, Southampton, United Kingdom
(Received 23 February 1994)

We make a theoretical study of the chevron and tilted structures in the smectic-A phase of a liquid crystal. These structures have been observed to occur in cells in which the director is oriented in the plane of the wall. We examine the hypothesis of Limat and Prost [Liq. Cryst. **13**, 101 (1993)] that the layer buckling and the tilting is a consequence of a mismatch between layer thickness in the bulk and at the surface. We use the covariant form of the Landau–de Gennes free energy expressed in terms of the nematic director field $\mathbf{n}(\mathbf{r})$ and the smectic complex order parameter $\psi(\mathbf{r})$. The threshold condition for and evolution of the chevron and tilted structure are obtained as a function of liquid crystal elastic properties, cell thickness, and surface orientational anchoring strength. The threshold and amplitude evolution exhibit almost universal behavior as a function of a dimensionless chevron number σ. We give a possible explanation of the hysteresis effect observed in the liquid crystal 4O.8 [4-octyl-*n*-(4′-butoxybenzylidene)aniline]. We estimate the energy barrier for the chevron–tilted-structure transition and discuss the case where the stress imposed by surface positional anchoring is partially relieved by incorporating a lattice of wedge dislocations.

PACS number(s): 61.30.Eb, 61.30.Cz, 83.70.Jr

I. INTRODUCTION

Recently there have been many studies of smectic liquid crystals (LC's) confined between parallel bounding plates in the so-called bookshelf structure. In this structure the layers are perpendicular to the cell walls. An understanding of the stability of the bookshelf structure is of considerable importance in the development of display devices based on smectic LC technology. The perfect bookshelf geometry in practice, however, only rarely occurs. More often the so-called chevron structure, shown in Fig. 1, is seen. In this case the smectic layers are symmetrically tilted, with a kink in the middle of the cell.

The chevron structure is believed to be the consequence of the mismatch between the natural smectic layer separation d_0 and the separation d_s imposed by the surface interaction [1–7]. If $d_s > d_0$, by tilting the layers, the smectic liquid crystal can avoid the strong elastic deformations, uniformly distributed over the whole cell, which retaining planar bookshelf geometry would imply. The tilt compensates the difference between d_s and d_0, the tilt angle thus tends to the value $\theta_m = \cos^{-1}(d_0/d_s)$. The resulting structure is energetically favorable compared to the bookshelf configuration. The elastic deformations are now localized at the boundary plates and in the middle of the cell. In detail, the chevron structure depends on the interplay between elastic nematic, smectic, and surface interaction forces.

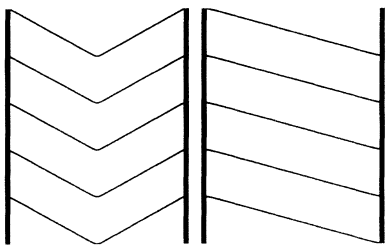

FIG. 1. Schematic representation of the chevron (left) and tilted (right) structures, showing the structure of the smectic layers within a cell. In the Sm-A phase the nematic molecules tend to be oriented along the layer normal.

The chevron structure was first observed in a ferroelectric smectic-C LC by Rieker *et al.* [1]. There has been much subsequent experimental and theoretical investigation [2–4] of the mechanism of chevron formation. Recently the chevron configuration has also been observed by Takanishi and co-workers [5,6] in the smectic-A (Sm-A) phase. Although this phase seems to be less relevant in a commercial context, it is a particularly simple model which may nevertheless serve as a paradigm for the investigation of chevron formation in general. The structure of a Sm-A LC is less complex than that of a Sm-C LC. It is therefore easier to extract the crucial parameters for chevron formation. In a subsequent study we shall show how our results may be naturally extended to Sm-C materials.

We begin with a brief summary of the main experimental features of the chevron structure in the Sm-A phase. X-ray patterns [5,6] reveal the continuous onset of chevron ordering on cooling from the nematic (N) phase. For some samples the data show pronounced thermal hysteresis. The experiments also indicate that, for small cell thickness, the chevron structure is replaced by a tilted structure, also shown in Fig. 1. In this structure the smectic layers simply tilt to satisfy the positional bound-

*Permanent address: Faculty of Education, Department of Physics, University of Maribor, Slovenia.

ary conditions. This requires slipping of smectic layers at the bounding plates. The amplitude of the tilted structure shows continuous development on cooling from the nematic phase. Takanishi and co-workers [5,6] suggest that the observed continuous chevron and tilted structure evolution results from layer thinning. This conclusion is based on the experimental observation that the thickness of smectic layers reduces with decreasing temperature.

Two theoretical studies [3,7] have concentrated on the chevron structure in the Sm-A phase. Nakagawa [3] has proposed a simple soliton model to model the chevron layer structure in smectic phases. He demonstrates that a coupling between the layer compression and the density change at the Sm-A–nematic phase transition can cause chevron formation. A more detailed study of the chevron structure in the Sm-A phase has been carried out by Limat and Prost [7]. They express the free energy density in terms of the smectic layer tilt angle and the strain $\epsilon=d_s/d_0-1$ imposed by the bounding plates. They show that the chevron structure in a cell of thickness L exists only for a strain larger than a threshold value $\epsilon_c \propto (L/\lambda)^2$, where λ is the smectic penetration depth. The chevron structure evolves continuously for $\epsilon > \epsilon_c$. They propose two mechanisms for the chevron formation on cooling from the nematic phase: (i) the layer thinning effect discussed above, and (ii) the strong temperature dependence of λ near the N–Sm-A transition at constant strain. They find that the threshold value for the existence of the tilted structure is $\epsilon_c/4$.

In this article we extend the study of Limat and Prost to a more general case. We use the covariant form of the Landau–de Gennes free energy in terms of the nematic director field $\mathbf{n}(\mathbf{r})$ and the smectic complex order parameter $\psi(\mathbf{r})$. The plan of the paper is as follows. In Sec. II the model free energy and corresponding Euler-Lagrange equations are presented. In Sec. III we study the influence of LC bulk elastic properties on the chevron evolution in the strong anchoring regime. The effect of weak director anchoring is studied in Sec. IV. A possible scenario for the hysteresis effects observed in the 40.8 [4-octyl-*n*-(4′-butoxybenzylidene)aniline] LC is discussed in Sec. V. In Sec. VI we estimate the energy barrier for the chevron–tilted-structure transition. In Sec. VII we compare the chevron structure with a structure incorporating edge dislocations. In the last section we draw some brief conclusions. We discuss in an Appendix the relationship between our work and that of Limat and Prost.

II. MODEL

In our study the chevron structure in the Sm-A phase is described in terms of the nematic director field $\mathbf{n}$ and the smectic density wave $\psi=\eta e^{i\phi}$. The unit vector $\mathbf{n}$ points along the average local orientation of a LC molecule. The smectic translational order parameter η describes the degree of smectic ordering and the phase factor ϕ determines the position of a smectic layer. In terms of these parameters the covariant form of the Landau–de Gennes free energy [8–11] is expressed as

$$\int f(\mathbf{r})d^3\mathbf{r}=\int [f_n(\mathbf{r})+f_s(\mathbf{r})]d^3\mathbf{r}+\int f_a(r)d^2\mathbf{r} \ . \tag{1}$$

The nematic $f_n(\mathbf{r})$, smectic $f_s(\mathbf{r})$, and surface anchoring $f_a(\mathbf{r})$ free energy density contributions are given by

$$f_n(\mathbf{r})=\frac{K_{11}}{2}[\nabla\cdot\mathbf{n}(r)]^2+\frac{K_{22}}{2}(\mathbf{n}\cdot\nabla\times\mathbf{n})^2 + \frac{K_{33}}{2}(\mathbf{n}\times\nabla\times\mathbf{n})^2 \ , \tag{1a}$$

$$f_s(\mathbf{r})=\gamma_{\parallel}|(\mathbf{n}\cdot\nabla-iq_0)\psi|^2+\gamma_{\perp}|(\mathbf{n}\times\nabla)\psi|^2 \ , \tag{1b}$$

$$f_a(\mathbf{r})=\frac{W_0}{2}(\mathbf{n}\cdot\boldsymbol{\nu})^2 \ . \tag{1c}$$

Here K_{11}, K_{22}, and K_{33} denote the nematic splay, twist, and bend elastic constants, respectively. The quantities $\gamma_{\parallel}$ and $\gamma_{\perp}$ are smectic elastic constants which describe, respectively, the layer compressibility and the cost of tilting the director with respect to the layer normal. The $\gamma_{\parallel}$ term favors the formation of a density wave in the $\mathbf{n}$ direction with the layer spacing $d_0=2\pi/q_0$. The orientational anisotropic part of the substrate-LC interaction is modeled by a term weighted by the anchoring strength constant W_0, which tends to orient the director at the surface perpendicular to the surface normal $\boldsymbol{\nu}$. This kind of boundary condition is conventionally called planar anchoring.

The bend and twist elastic constants exhibit divergent behavior on approaching a second order N–Sm-A transition from above as a result of smectic pretransitional fluctuations [12]. These fluctuations introduce into the nematic phase small domains with local smectic organization. Since the Sm-A phase is incompatible with twist and bend nematic deformation, the presence of smectic domains gives rise to an anomalous increase in measured values of the elastic constants K_{22} and K_{33}. However, in the smectic phase K_{22} and K_{33} need not be considered to have infinite value. The nematic bend and twist deformation are forbidden by the topology of the smectic phase itself. The nematic elastic constants in Eq. (1) may be considered to be "bare" nematic elastic constants in the sense that they do not include smectic phase fluctuations.

The calculations are performed in the Cartesian coordinate system $\mathbf{r}=(x,y,z)$. The Sm-A liquid crystal is confined between two plates located at $x=-L/2$ and $x=L/2$ and the layers are running in the z direction. We confine our interest to the case when the mismatch between LC and surface positional smectic layer configuration is resolved by tilting the layers. This allows us to restrict $\mathbf{n}$ to lie in the (x,z) plane: $\mathbf{n}=(\sin\theta,0,\cos\theta)$. Here $\theta(x)$ denotes the angle between $\mathbf{n}$ and the z axis. For such a director configuration the K_{22} term in Eq. (1) vanishes. We enforce the smectic density wave in the z direction by taking ψ to be of the form

$$\psi(\mathbf{r})=\eta e^{iq[z+u(x)]} \ , \tag{2}$$

where the displacement field $u(x)$ describes departures from the planar layer configuration. The wave vector q is in general different from q_0. It is imposed by the surface which enforces smectic layer separation $d_s=2\pi/q$. In this model we assume strong smectic positional anchoring and the layers are not allowed to slip or form disloca-

tions. In addition we neglect the spatial variations of η.

The most relevant quantities of our study are (i) the strain $\epsilon=1-q/q_0$ imposed on the LC because $q\neq q_0$, (ii) the penetration depth $\lambda_\perp=\sqrt{K_{33}/(\gamma_\perp q_0^2\eta^2)}$, measuring how far into the smectic phase the bend nematic deformation persists, and (iii) the surface extrapolation length $\lambda_s=K_{11}/W_0$, describing the influence of the surface anchoring on the $\mathbf{n}$ profile. The chevron structure can exist if $\lambda_\perp<L$. The surface anchoring strength plays an important role if $L/\lambda_s>1$. We write our equations in terms of the dimensionless quantities $a_3=K_{33}/K_{11}$, $a=\gamma_\perp/\gamma_\parallel$, $w=\partial u/\partial x$, and $\rho=x/L$. For calculational convenience we introduce a parameter $\lambda=\lambda_\perp\sqrt{a/a_3}$. With these definitions we can compute a dimensionless free energy G per unit surface:

$$G=\frac{L}{K_{11}}\int_{-L/2}^{L/2}f(\mathbf{r})dx$$
$$=\int_{-1/2}^{1/2}[g_n(\rho)+g_s(\rho)]d\rho+g_a(\tfrac{1}{2})+g_a(-\tfrac{1}{2})\ . \tag{3}$$

Here

$$g_n(\rho)=\frac{1}{2}\left[\frac{\partial\theta}{\partial\rho}\right]^2(\cos^2\theta+a_3\sin^2\theta)\ , \tag{3a}$$

$$g_s(\rho)=\frac{L^2}{\lambda^2}\{a(w\cos\theta-\sin\theta)^2(1-\epsilon)^2$$
$$+[(1-\epsilon)(w\sin\theta+\cos\theta)-1]^2\}\ , \tag{3b}$$

$$g_a(\rho)=\frac{L}{\lambda_s}\frac{\sin^2\theta(\rho)}{2}\ . \tag{3c}$$

We can easily extract some asymptotic information about the chevron structure from Eq. (3b). The first term, describing the bend smectic elastic deformation, vanishes if $w=\tan\theta$. This condition sets nematic molecules perpendicular to smectic layers, which is shown in Fig. 2.

The condition $w=\tan\theta$ can be written in the form

$$\mathbf{n}=\nabla\phi/|\nabla\phi|=\{w,0,1\}/\sqrt{1+w^2}\ ,$$

and is in fact a requirement of the continuum theory approach [13] everywhere (not just in asymptotia). In this approach the Sm-A behavior is determined by the displacement field $u(\mathbf{r})$ alone, and $\mathbf{n}(r)$ is locked along the layer normal. The condition $w=\tan\theta$ is strictly realized within the Landau–de Gennes theory, however, only in the limit $\gamma_\perp\rightarrow\infty$.

The second term in Eq. (3b) is due to layer compressibility. It vanishes if, in addition to $w=\tan\theta$, $\cos\theta=1-\epsilon$ is also satisfied. This is the condition that smectic layers must be tilted at an angle $\theta=\theta_m\equiv\cos^{-1}(1-\epsilon)$ in order to preserve the equilibrium layer spacing. This condition can be also obtained by geometrical considerations alone, as can be seen in Fig. 2.

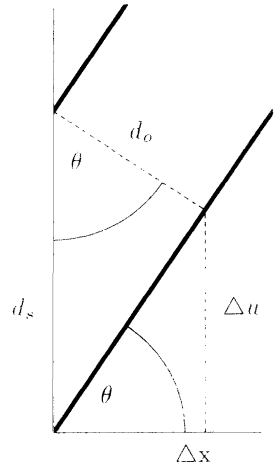

FIG. 2. The conditions $w=du/dx=\tan\theta$ and $\cos\theta=1-\epsilon=d_0/d_s$ minimizing the smectic elastic contribution can be extracted from geometrical considerations. The condition $w=\tan\theta$ sets nematic molecules along the smectic layer normal. Smectic layers tend to tilt at an angle $\theta=\cos^{-1}(d_0/d_s)$ in order to satisfy the surface anchoring imposing periodicity d_s and smectic elastic forces favoring the layer separation d_0.

In order to minimize this free energy we need to obtain the appropriate Euler-Lagrange equations. These are

$$\frac{\partial g_n}{\partial\theta}+\frac{\partial g_s}{\partial\theta}-\frac{\partial}{\partial\rho}\frac{\partial g_n}{\partial(\partial\theta/\partial\rho)}=0\ , \tag{4a}$$

$$\frac{\partial}{\partial\rho}\frac{\partial g_s}{\partial w}=0\ , \tag{4b}$$

$$\left\{-\frac{\partial g_n}{\partial(\partial\theta/\partial\rho)}+\frac{\partial g_a}{\partial\theta}\right\}_{(\rho=-1/2)}=0\ , \tag{4c}$$

$$\left\{\frac{\partial g_n}{\partial(\partial\theta/\partial\rho)}+\frac{\partial g_a}{\partial\theta}\right\}_{(\rho=1/2)}=0\ . \tag{4d}$$

Equations (4a) and (4b) come from the bulk contribution to the free energy. Equations (4c) and (4d) are boundary conditions. After some algebra these equations can be simplified, yielding

$$w=\tan(\theta)H(a,\rho)\ , \tag{5a}$$

$$-\frac{\partial^2\theta}{\partial\rho^2}(\cos^2\theta+a_3\sin^2\theta)+\left[\frac{\partial\theta}{\partial\rho}\right]^2(1-a_3)2\sin\theta\cos\theta+\frac{4(L^2/\lambda^2)a[1-(1-\epsilon)/\cos\theta][-1+(1-\epsilon)(1-a)\cos\theta]\sin2\theta}{[1+a+(a-1)\cos(2\theta)]^2}=0\ , \tag{5b}$$

$$\left[-\frac{\partial\theta}{\partial\rho}(\cos^2\theta+a_3\sin^2\theta)+\frac{L}{\lambda_s}\sin\theta\cos\theta\right]_{\rho=-0.5}=0\ , \tag{5c}$$

$$\left[+\frac{\partial\theta}{\partial\rho}(\cos^2\theta+a_3\sin^2\theta)+\frac{L}{\lambda_s}\sin\theta\cos\theta\right]_{\rho=0.5}=0\ , \tag{5d}$$

where

$$H(a,\rho)=\frac{(a-1)\cos^2\theta+\cos\theta/(1-\epsilon)}{(a-1)\cos^2\theta+1} . \tag{5e}$$

Equation (5a) yields a relation between the variational parameters of our approach, namely, $u(\mathbf{r})$ and $\theta(\mathbf{r})$. In the continuum theory approach, by contrast, $w=\tan\theta$ exactly. Therefore the quantity $H(a,\rho)$ can be used to measure departures from the continuum approximation. In Eq. (5b) we have already substituted for w in order to obtain an equation in terms of θ alone.

The boundary conditions for $\theta(\rho)$ are defined by Eqs. (5c) and (5d). In the case of strong anchoring ($W_0\to\infty$) they enforce $\theta(\pm\frac{1}{2})=0$. For $W_0=0$ we have $\partial\theta/\partial\rho(\pm\frac{1}{2})=0$. The strain $\epsilon=1-q/q_0$ is imposed by surface positional anchoring. In our model strong positional anchoring is assumed, which enforces the smectic layer separation $d_s=2\pi/q$ at the boundary plates.

The equations are solved numerically using the relaxation method [14]. The layer displacement $u(\rho)$ is obtained from $w(\rho)$ by integration.

III. CHEVRON STRUCTURE

Previous experimental and theoretical results suggest that the chevron structure in the Sm-A phase can exist only if a threshold condition is exceeded [5–7]. The way the chevron evolves from the bookshelf structure is reminiscent of the familiar Freedericks transition [9,12] in a thin nematic layer. In a conventional arrangement the nematic LC is confined between parallel plates enforcing homeotropic anchoring. An external (electric or magnetic) field $\mathbf{h}$ is applied in a direction perpendicular to the plate normal. The field $\mathbf{h}$ is thus in competition with nematic elastic forces which favor the homogeneous structure imposed by the boundary conditions. The field can continuously break this ordering if the field strength exceeds a threshold value h_c. In the chevron case it is the strain ϵ which tends to break the homogeneous planar Sm-A ordering imposed by the smectic elastic constants.

To obtain analytically the threshold condition and the amplitude of the chevron structure one can directly follow the mathematical procedure developed for the Freedericks transition by Vertogen and de Jeu [9]. We present here an alternative derivation based on free energetic arguments. Our main conclusions are as follows.

(i) The onset of the chevron and tilted structures can be parametrized by a single dimensionless parameter which we shall call the chevron number σ, defined by

$$\sigma=\frac{\epsilon L^2}{2\pi^2\lambda^2}\left[1+\epsilon\left[\frac{\gamma_\parallel}{\gamma_\perp}-1\right]\right] . \tag{6}$$

The chevron structure exists for

$$\sigma\geq\sigma_c . \tag{6a}$$

The tilted structure can occur if

$$\sigma\geq\sigma_t . \tag{6b}$$

For strong anchoring $\sigma_c=1$, $\sigma_t=\frac{1}{4}$.

(ii) The evolution of the chevron and tilted structures also exhibits almost universal behavior as a function of σ. For conventional values of LC material parameters the scaled chevron–tilted-structure amplitude behaves to a good approximation as

$$\frac{\theta_i}{\theta_m}\sim\left[\frac{\sigma-\sigma_i}{\sigma}\right]^{1/2} , \tag{7}$$

where the indices $i=\{c,t\}$ denote the chevron–tilted structure and $\theta_m=\cos^{-1}(1-\epsilon)$ is the asymptotic amplitude of both structures.

A. The chevron transition

The chevron transition can be examined using a Landau-type theory. Since w can be expressed in terms of θ via Eq. (5a) only θ need be taken into account. We expand the free energy density given in Eq. (3) up to fourth order in θ. The chevron structure requirement $\theta(0)=0$ and the boundary condition $\theta(-0.5)=\theta(0.5)=0$ imply that θ can be written as

$$\theta=\sum_{k=1}^{\infty}\theta_c^{(k)}\sin(2k\pi\rho)\sim\theta_c^{(1)}\sin(2\pi\rho) , \tag{8}$$

where the leading term $\theta_c^{(1)}$ dominates close to the transition. The resulting dimensionless free energy in terms of the mode amplitude is

$$G=G_{\text{book}}-\frac{\alpha(\theta_c^{(1)})^2}{2}+\frac{\beta(\theta_c^{(1)})^4}{4} . \tag{9}$$

The quantity $G_{\text{book}}=(L^2/\lambda^2)\epsilon^2$ describes the bookshelf geometry distortion free energy and α,β are expansion constants given by

$$\alpha=-2\pi^2+\frac{L^2}{\lambda^2}\left[\epsilon+\left[\frac{1}{a}-1\right]\epsilon^2\right]$$
$$=2\pi^2(\sigma-1)=2\pi^2(\sigma-\sigma_c) , \tag{9a}$$

$$\beta=(-1+a_3)\pi^2+\frac{3L^2}{2\lambda^2}\left[\frac{1}{4}+\left[-\frac{11}{12}+\frac{1}{a}\right]\epsilon+\left[\frac{2}{3}+\frac{1}{a^2}-\frac{5}{3a}\right]\epsilon^2\right] . \tag{9b}$$

The bookshelf structure is destabilized with respect to the chevron structure when $\alpha\geq 0$, yielding the threshold condition Eq. (6a) for chevron formation. The chevron structure is preferred by thick cells, strong strain ϵ, high ratio $\gamma_\parallel/K_{11}$, and high smectic order parameter. At the continuous N–Sm-A transition, when $T=T_{NA}$, $\eta(T_{NA})=0$, and hence σ tends to zero.

We note at this stage that experimentally [5,6] $\epsilon<0.01$, and it is convenient to consider ϵ as a small parameter in the expressions that follow.

Now the mode amplitude $\theta_c^{(1)}$ is determined from $\partial G/\partial\theta_c^{(1)}=0$, yielding

$$\theta_c^{(1)}=\left[\frac{\sigma-\sigma_c}{\frac{3\sigma}{2\epsilon\{1+\epsilon[(1/a)-1]\}}\left[\frac{1}{4}+\left[-\frac{11}{12}+\frac{1}{a}\right]\epsilon+\left[\frac{2}{3}+\frac{1}{a^2}-\frac{5}{3a}\right]\epsilon^2\right]+\frac{\sigma_c(a_3-1)}{2}}\right]^{1/2} \tag{10}$$

However,

$$\theta_m=\cos^{-1}(q/q_0)=\cos^{-1}(1-\epsilon)\sim\sqrt{2\epsilon}\ .$$

If we factor out θ_m in this equation, what remains contains terms of $O(1)$, $O(\epsilon)$, and $O(\epsilon^2)$. For small ϵ the terms of $O(1)$ usually dominate. When this is the case Eq. (10) reduces to

$$\theta_c^{(1)}\sim\theta_m\left[\frac{4(\sigma-\sigma_c)}{3\sigma}\right]^{1/2}\ . \tag{10a}$$

In this form $\theta_c^{(1)}/\theta_m$ is a universal function of the chevron number σ. Terms of $\theta(\epsilon)$ play the leading role in departures from universality. These corrections have contributions from $a_3=K_{33}/K_{11}$ and $a=\gamma_\perp/\gamma_\parallel$. The latter contributions enter in the form $1/a$, and this quantity diverges at the Sm-A–Sm-C transition [10]. We therefore expect that there may be departures from universality in this region of the phase diagram.

We note that Eq. (10a) differs from Eq. (7) by a factor of ~ 1.16; the wrong maximal tilt is predicted. However, this approximation only considers the leading sinusoidal contribution to the full chevron profile. For large σ the chevron profile changes from a sinusoidal to a solitonlike form. In fact, it is surprising that in the Landau theory such a good result is obtained. Nevertheless, we expect the conclusions about universality to be more generally true.

In the case $\gamma_\parallel=\gamma_\perp$ the threshold condition simplifies to $\sigma_c=\sigma_0$, where

$$\sigma_0=\frac{\epsilon\gamma_\parallel q_0^2\eta^2L^2}{2\pi^2K_{11}}=\frac{\epsilon L^2}{2\pi^2\lambda^2}\ . \tag{11}$$

This condition is equivalent to the result of the Limat-Prost approach [7]. In the Appendix we discuss in more detail the relationship between our calculations and those of Limat and Prost. Recent experiments [5,6] suggest that $\epsilon<0.01$. Hence for conventional circumstances the condition $\sigma\sim\sigma_0$ holds, except near the Sm-A–Sm-C transition.

The chevron free energy close to the threshold in the limit $\epsilon\ll 1$ is given by

$$G-G_{\text{book}}=-\frac{\alpha^2}{4\beta}\sim-\frac{2\pi^2\theta_m^2}{3}\frac{(\sigma-\sigma_c)^2}{\sigma}\ . \tag{12}$$

The strain imposed by the surface mismatch can also be depressed by formation of the tilted structure shown in Fig. 1. In this structure the smectic layers tend to be tilted at the angle θ_m to satisfy the positional boundary condition. The elastic deformations are localized at the substrate-LC interface. In the strong anchoring regime the free energy of the tilted structure is approximately half the free energy of the chevron structure [7]. However, the tilted structure requires the smectic layers to slip at the interface. Experiments [5,6] suggest that slipping is either sufficiently energetically costly or sufficiently slow that chevron formation is preferred. Only in the regime where the chevron structure cannot exist does the tilted structure occur [6,7]. In particular, it persists below σ_c, because of its lower deformational free energy.

To study the lower limits of the tilted structure existence we follow the same procedure as for the chevron structure, lifting the layer nonslip constraint. In this case θ can be expressed as

$$\theta=\sum_{k=1}^{\infty}\theta_c^{(k)}\sin(2k\pi\rho)+\sum_{k=0}^{\infty}\theta_t^{(k)}\cos[(2k+1)\pi\rho]\ .$$

The mode that first destabilizes the bookshelf structure is now $\theta_t^{(0)}\cos(\pi\rho)$. This occurs when condition Eq. (6b) is fulfilled. The corresponding amplitude $\theta_t^{(0)}$ evolves according to Eq. (10) if we replace σ_c by σ_t.

B. The chevron structure at high chevron number

In order to study the chevron structure for arbitrary values of model parameters we have carried out a numerical study of the solutions of Eqs. (5). The chevron structure in different stages of development is shown in Fig. 3. With increasing σ, the structure of $\theta(\rho)$ changes from a sinusoidal to a solitonlike solution. For $\sigma\gg 1$ the chevron amplitude approaches $\theta_m=\cos^{-1}(1-\epsilon)$. Just beyond the chevron transition the elastic distortions are spread across the whole cell. For higher values of the chevron number the distortions become localized at the substrate-LC interface and in the middle of the cell. This is evident from the plot of the elastic free energy density $g(\rho)$, shown in Fig. 3(c).

In Fig. 3(d) the deviation of our model from the continuum approach is shown. The deviations are strongest in the middle of the cell and at bounding plates where the elastic deformations are large. The maximal deviation is given by $H(a,0)=[a-1+1/(1-\epsilon)]/a$. For the case of equal smectic elastic constants it simplifies to $H(1,0)=1/(1-\epsilon)$. We see that for $\epsilon<0.01$ (the regime in which recent experiments were carried out) the continuum approach is excellent since maximal departure is less than 1%.

The evolution of the chevron and tilted structure ordering is demonstrated in Fig. 4, in which we plot the spatial dependence of θ_c/θ_m and θ_t/θ_m. The amplitudes are given by $\theta_c=\theta(\rho=\frac{1}{4})$ and $\theta_t=\theta(\rho=0)$, where $\theta(\rho)$ denotes the chevron or tilted director profile. Note the onset of chevron structure at $\sigma=\sigma_c\equiv 1$ and the tilted structure at $\sigma=\sigma_t\equiv\frac{1}{4}$. For $\sigma<\sigma_t$ only the bookshelf structure can exist. Our numerical studies confirm the analytical conclusions that it is essentially only the chevron number σ which determines the chevron structure. In Fig. 4 we show the effect of a variation in the parameter $a_3=K_{33}/K_{11}$ on the behavior of θ_c/θ_m. The relative

deviations from the curves shown caused by a choice of different $\gamma_{\parallel}/\gamma_{\perp}$ or ϵ values are much weaker.

IV. WEAK ANCHORING

The results of the previous section are valid in the case of strong anchoring, in which the surface director orientation is constrained to be planar. In the case of weak anchoring the director field at the LC-substrate interface is allowed to come out of the surface plane. The final director orientation is now a compromise between LC elastic and anchoring forces.

There are two physical effects which follow from the possibility of weak anchoring. First, the departure of θ from the easy direction, which minimizes the anchoring term, reduces the distortion field at the bounding plates. Thus for very weak anchoring the major contribution to the elastic free energy is localized in the center of the cell. Secondly, in the weak anchoring regime it is easier for the LC to deform its structure at the LC-substrate interface. The strain threshold value for the chevron formation is thus depressed. The lower limit of $\sigma_c(W_0)=\sigma_c(W_0=0)$ can easily be obtained analytically. For $W_0=0$ the boundary conditions read $\partial\theta/\partial\rho(-0.5)=\partial\theta/\partial\rho(0.5)=0$, allowing $\theta=\sum_{k=1}^{\infty}\theta_c^{(k)}\sin(k\pi\rho)$. The lowest energy mode, which destabilizes the bookshelf structure, is then $\theta=\theta_c^{(1)}\sin(\rho\pi)$, corresponding to the threshold condition $\sigma=\sigma_c(0)=\frac{1}{4}$. The amplitude $\theta_c^{(1)}\sim\theta_c$ obeys Eq. (10) where $\sigma_c=\sigma_c(0)$.

It is convenient to have a nondimensional measure of the anchoring strength W_0. In practice it is more useful to work with the surface extrapolation length $\lambda_s \propto 1/W_0$, which is zero at strong anchoring. We define the quantity $\mu=\lambda_s/L$ as a nondimensional measure of W_0.

In Fig. 5 we show a high σ chevron structure for

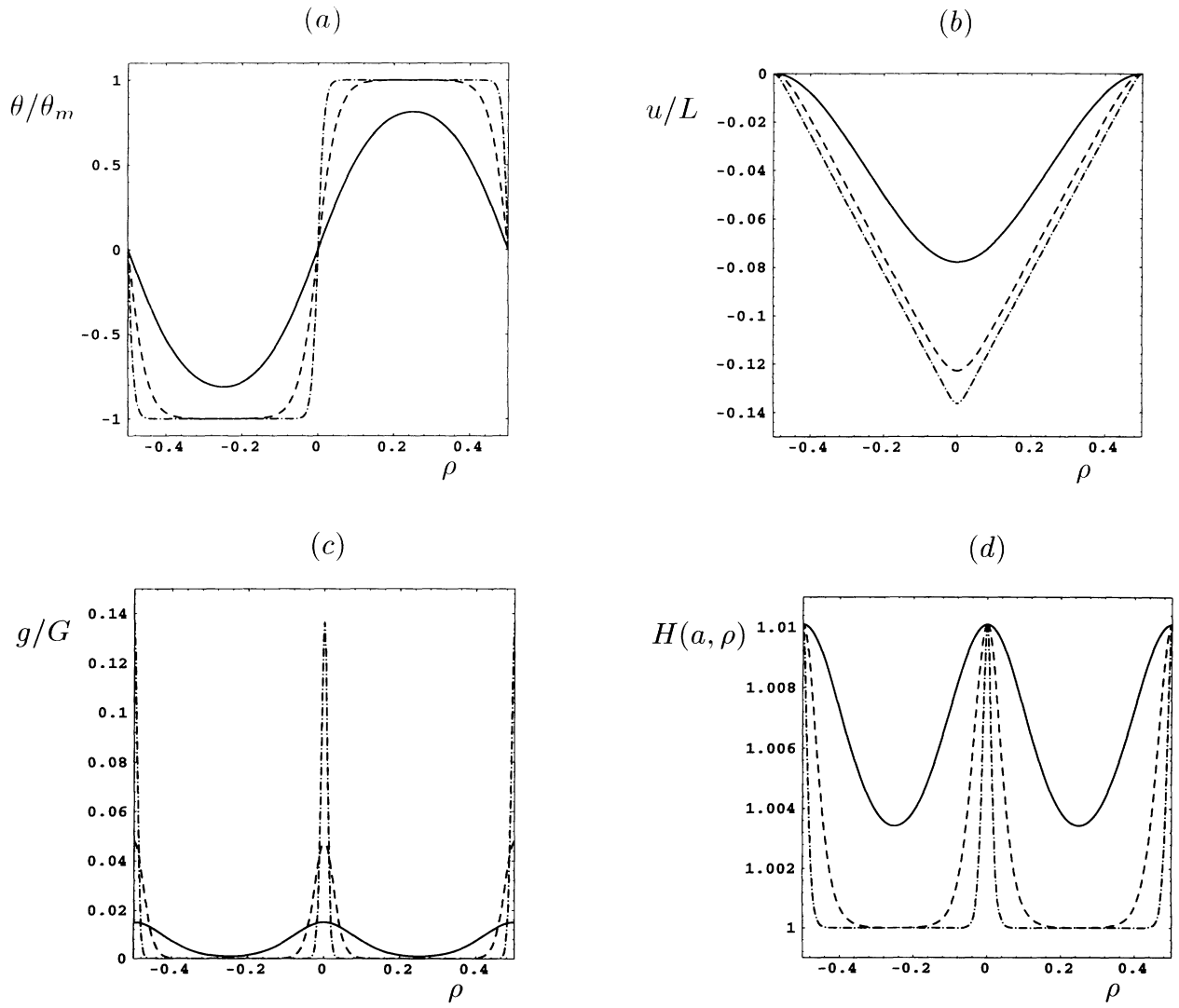

FIG. 3. The chevron structure for different values of the chevron number: (a) $\theta(\rho)/\theta_m$, (b) $u(\rho)$, (c) $g(\rho)/G$ [$G=\int g(\rho)d\rho$]. In (d) the departures $H(a,\rho)$ from the continuum approximation are shown in which $H(a,\rho)=1$. Full line: $\sigma=2$, dashed line: $\sigma=20$, dash-dotted line: $\sigma=200$. In all cases $a_3=a=1$, $\epsilon=0.01$, and $\lambda_s=0$, corresponding to strong anchoring.

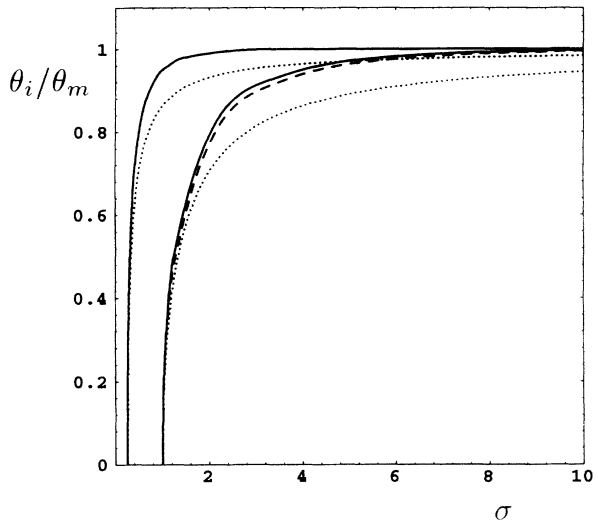

FIG. 4. The chevron and tilted structure evolution. Dependence of θ_i/θ_m on σ, $i=\{c,t\}$. Full line: $a=a_3=1$, $\epsilon=0.01$; dashed line: $a=1$, $a_3=10$, $\epsilon=0.01$. The dotted lines present the structure of the chevron and tilted structure amplitude in the case $a=a_3=1$, as predicted by the approximate universal curve given by Eq. (10). Strong anchoring.

several different anchoring strengths. In Fig. 6 we plot the threshold value $\sigma_i, i=\{c,t\}$, as a function of σ_s. As W_0 is decreased and μ is increased the critical chevron number drops from $\sigma_c(\infty)=1$ to $\sigma_c(0)=\frac{1}{4}$. We note also that the critical value for the tilted structure drops from $\sigma_t(\infty)=\frac{1}{4}$ to $\sigma_t(0)=0$. The significance of this last result is that if the director at the surface may reorient freely there is no longer any energy barrier to layer tilt, and consequently the critical chevron number goes to zero.

V. THERMAL HYSTERESIS

There are experiments which suggest that the chevron and tilted structures in some circumstances experience thermal hysteresis behavior [5,6]. This seems to depend on the LC phase sequence, the cell thickness, and the thermal history of the sample. In this section we show that the surface memory effect (SME) [15] may be responsible for some of these observations.

Ouchi *et al.* [6] have studied chevron structure as a function of temperature in the liquid crystal 4O.8. In a thick cell ($L\sim 25$ μm) chevron onset occurs at $T=T_c(L)$ on cooling, and at $T=T_h(L)$ on heating, with $T_c(L)<T_h(L)\sim T_{NA}$. The chevron amplitude on heating is approximately twice the amplitude on cooling. As T is decreased there is a phase transition from Sm-A to Sm-B phase. At the phase transition the chevron structure suddenly collapses and the bookshelf structure is reestablished. When the cell thickness is reduced the cooling chevron branch is only weakly influenced. By contrast, the chevron amplitude of the heating branch is drastically reduced and $T_h(L)$ becomes apparently lower than $T_c(L)$.

This behavior can be partly explained in the following

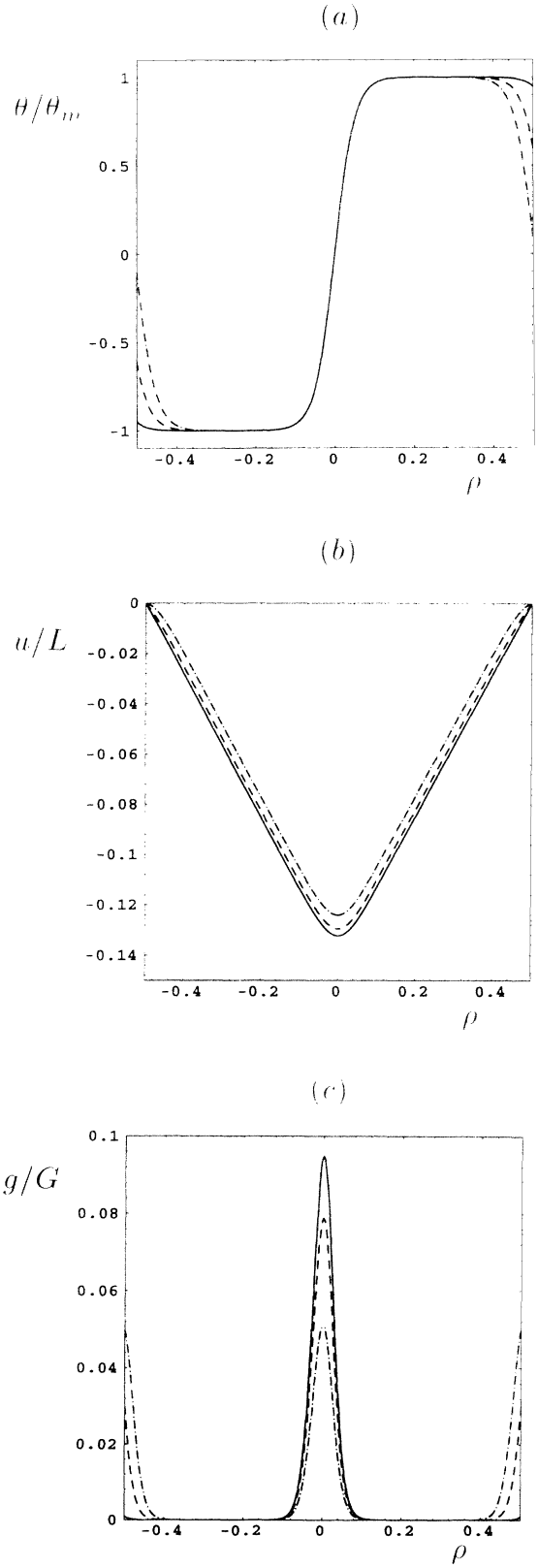

FIG. 5. The chevron structure for different orientational anchoring strengths: (a) $\theta(\rho)/\theta_m$, (b) $u(\rho)$, (c) $r(\rho)=g(\rho)/G$ $[G=\int g(\rho)d\rho]$. Full line: $L/\lambda_s=1$; dashed line: $L/\lambda_s=10$; dash-dotted line: $L/\lambda_s=100$. In all cases $L^2/\lambda^2=10^4$, $a=a_3=1$, $\epsilon=0.01$, and $\sigma=20$.

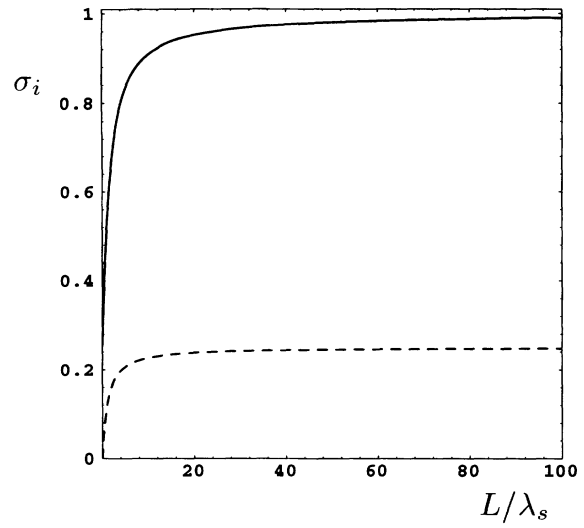

FIG. 6. The effect of the surface anchoring strength on onset σ_i of the chevron ($i=c$) and tilted ($i=t$) structures in the case $a=a_3=1$. Full line: chevron; dashed line: tilted structure.

way. Following Durand [16] and Cagnon and Durand [17], we believe that the surface positional ordering with periodicity q is not an inherent property of bounding plates. But wetting the plates with a smectic phase induces a "fingerprint" surface periodicity. This picture is consistent with observations of Rieker *et al.* [1], who find that the chevron tilt angle is almost independent of the surface treatment.

Our model of the hysteresis phenomenon is as follows. On entering the Sm-A phase on cooling, the smectic bookshelf layered structure establishes a surface potential of periodicity $d_s=d_0(T_{NA})\sim 2.8044$ nm. Let us assume that on cooling the intrinsic smectic layer thickness $d_0(T)$ shrinks, as is indicated by x-ray data [6]. However, if the smectic compressibility constant is not large enough it is not possible during the experiment to rearrange the surface periodicity to match the new minimal free energy bulk bookshelf configuration. The surface positional ordering is frozen in with periodicity d_s. The discrepancy between d_s and $d_0(T)$ imposes strain

$$\epsilon_c(T)=1-d_0(T)/d_s=1-d_0(T)/d_0(T_{NA}) .$$

The chevron structure forms when the condition $\sigma=\sigma_c$ is satisfied. Near the threshold a maximal chevron tilt angle θ_m is strongly dependent on $\epsilon[\theta_m(\epsilon\ll 1)\sim\sqrt{2\epsilon}]$. Thus even a relatively small imposed strain can cause a pronounced chevron tilt. Once the chevron structure is formed, the tendency of the liquid crystal to rearrange the surface periodicity is decreased.

We now estimate $T_c(L)$ corresponding to the chevron onset condition. We assume the following simplification in the Sm-A phase: (i) we suppose strong anchoring, $\lambda_s=0$; (ii) we set $\gamma_\parallel=\gamma_\perp=\gamma$, (iii) we assume that close to T_{NA} $\eta(T)\sim\eta_0\sqrt{(T_{NA}-T)/T_{NA}}$, and (iv) the layer thickness shrinks linearly with temperature: $d_0(T)=d_0(T_{NA})-\delta(T_{NA}-T)$. The strain $\epsilon(T)$ is now given by $\epsilon\sim\delta(T_{NA}-T)/d_0(T_{NA})$. We introduce the quantity $\lambda_0=\lambda\eta=\sqrt{K_{11}/(\gamma_\parallel q_0^2)}$, whose temperature variation can be neglected. The chevron forms when

$$\sigma=\epsilon L^2\eta^2/(2\pi^2\lambda_0^2)$$
$$=(T_{NA}-T_c)^2\delta L^2\eta_0^2/(T_{NA}d_0 2\pi^2\lambda_0^2)=1 , \quad (13a)$$

yielding

$$\Delta T_c=T_{NA}-T_c=\frac{\pi\lambda_0}{\eta_0 L}\left[\frac{2T_{NA}d_0}{\delta}\right]^{1/2}$$
$$=T_{NA}\frac{2\pi^2\lambda_0^2}{\epsilon_c(T_c)\eta_0^2L^2} , \quad (13b)$$

where ϵ_c describes the strain ϵ at $T=T_c$.

On entering the Sm-B phase K_{11} and hence λ_0 diverges [18]. The chevron number

$$\sigma\sim\sigma_0=(\epsilon\gamma_\parallel q_0^2\eta^2L^2)/(2\pi^2K_{11})$$

drops abruptly to zero. Now $\sigma<\sigma_c$ and the chevron structure is replaced by the bookshelf geometry. In the Sm-B phase the equilibrium smectic layer spacing suddenly increases [6] to $d=d_B\sim 2.8317$ nm. The compressibility in the Sm-B phase is larger than in the Sm-A phase. If it is large enough it rearranges the surface to exhibit periodicity $d_s\sim d_B$ minimizing the S_B bulk free energy, and in fact this does occur experimentally.

If the sample is then heated it reenters the Sm-A phase. However, because of the relatively weak layer compressibility in the Sm-A phase, it is the surface periodicity established in the Sm-B phase, with $d_s=d_B$, which is now frozen in. On heating the strain imposed is

$$\epsilon_h(T)=1-d_0(T)/d_B>\epsilon_c(T) .$$

In this case we neglect its temperature variation. The chevron onset requires

$$\sigma=\epsilon_h L^2\eta^2/(2\pi^2\lambda_0^2)$$
$$=\epsilon_h L^2\eta_0^2(T_{NA}-T_h)/(T_{NA}2\pi^2\lambda_0^2)=1 , \quad (13c)$$

yielding

$$\Delta T_h=T_{NA}-T_h=T_{NA}\frac{2\pi^2\lambda_0^2}{\epsilon_h\eta_0^2L^2} . \quad (13d)$$

Equations (13) are consistent with the following experimental observations for thick cells ($L>20$ μm): (i) since $\epsilon_h>\epsilon_c$ we expect $T_h>T_c$, (ii) for large L values $T_h\sim T_c\sim T_{NA}$, and (iii) $\theta_m(\epsilon_h)>\theta_m(\epsilon_c)$.

To estimate the temperature shift ΔT_c we set $\lambda_0\sim 2.5$ nm, $\eta_0\sim 1$, $\delta\sim 0.007$ nm/15 °C, $T_{NA}=63$ °C and $d_0\sim 3$ nm. For this reasonable choice of parameters [6,17,19] in a cell with $L=25$ μm we find the temperature shift $\Delta T_c\sim 0.5$ °C which is in agreement with the experimental result. The experimentally determined chevron amplitude evolution suggests

$$\theta_m(\epsilon_h)/\theta_m(\epsilon_c)\sim\sqrt{\epsilon_h/\epsilon_c}\sim 2 .$$

Therefore $\epsilon_h\sim 4\epsilon_c$ and

$$\Delta T_h(25\ \mu\text{m})/\Delta T_c(25\ \mu\text{m}) \sim \frac{\epsilon_c}{\epsilon_h} \sim \frac{1}{4}$$

in accordance with experiment.

With decreased cell thickness the chevron amplitude of the heating branch decreases and approaches the amplitude of the cooling branch. This suggest that the bulk Sm-B influence is losing its dominance over the surface positional ordering. This is understandable since the bulk elastic free energy of the bookshelf geometry is proportional to L while the surface interaction is independent of the cell thickness. The surface ordering is determined by a compromise between the Sm-B phase requiring d_B and the surface tendency to keep the memorized pattern $d_s \sim d_0(T_{NA})$. Experiment indicates that the latter influence becomes dominant at $L \leq 20\ \mu$m.

This competition in the Sm-B phase can be roughly studied by expressing the free energy per unit surface in the bookshelf geometry as

$$F(q) = \int_{-L/2}^{L/2} f(\mathbf{r})dx \sim L\gamma_B \eta^2 (q - q_B)^2 + W_p (q - q_f)^2 , \tag{14}$$

where q_f is the frozen-in periodicity at the surface, γ_B describes a compressibility in the Sm-B phase, and $q_B = 2\pi/d_B$. The second term in Eq. (14) models the surface positional anchoring. Its strength is measured by a constant W_p tending to match q with the frozen pattern $q_f \sim 2\pi/d_0(T_{NA})$. We can now define a length scale $\lambda_p = W_p/(\gamma_B \eta^2)$, and a dimensionless ratio $\kappa = L/\lambda_p$. If $\kappa \gg 1$ bulk effects should dominate, whereas if $\kappa \ll 1$ surface effects are stronger.

The value of q minimizing Eq. (14) is

$$q = \frac{q_B \kappa + q_f}{1 + \kappa} . \tag{15}$$

Thus, from Eq. (15) we see that for large values of κ the interface experiences periodicity $q \sim q_B$ and for small κ values $q \sim q_f$. We emphasize, however, that these considerations are only qualitative and do not in any sense constitute a detailed theory, which would require consideration of local potentials.

The picture outlined in Eqs. (13) no longer works for thin samples in which the periodicity is determined by the surface rather than by the bulk Sm-B phase. In fact experimentally this is also the case. For thick samples $\Delta T_c > \Delta T_h$, whereas for thin samples $\Delta T_c < \Delta T_h$. We do not have a detailed calculational scheme to describe this. However, we believe that the fact that substantially more defects are observed on heating than on cooling may be relevant. This may weaken the smectic phase, or equivalently η_0 may be reduced. Now from Eq. (13d) $T_h(L)$ will be reduced. The observed difference in the number of defects such as focal conics indicates that at any given temperature the configuration is subject to larger strain when it is heated. This is consistent with our numerical experience. We find that on approaching the $\sigma \sim \sigma_c$ regime the numerical calculations proceed extremely slowly, indicating a shallow potential. It seems possible that the experiment does not track the minimal energy configuration, at least close to σ_c. This "retardation" can cause a substantially more strained structure on heating than on cooling. The strain is partially relieved by defect formation.

VI. THE ENERGY BARRIER BETWEEN THE CHEVRON AND THE TILTED STRUCTURE

In our calculations the free energy of the tilted structure is always lower than that of the chevron structure. Experimentally, nevertheless, it seems that if the LC is subjected to strain ϵ it always adopts the chevron configuration. Only in the case that the chevron cannot exist ($\sigma < \sigma_c$) is the tilted structure realized. The realization of the tilted structure would require slipping of smectic layers at the LC-substrate interface. We believe that slipping causes rigid shifting of the surface positional ordering. The surface pattern follows the slipping of the LC, retaining periodicity q. This picture is consistent with the experimental observation [6] demonstrating continuous evolution of the tilted structure with temperature. Either the energy required for this process is very high or the slipping procedure is extremely slow. In any event chevron formation dominates.

In order to demonstrate that the formation of the tilted structure is very unlikely we estimate the upper bound of the energy barrier between the chevron and the tilted structure by considering another possible channel for the chevron-tilted transition. The chevron structure can continuously transform to the slipped structure via an intermediate state in which a part of the chevron structure is melted. This enables continuous rearrangement of parts separated by the melted region to the tilted structure. The most probable melting location is either the chevron tip or the interface region where the elastic deformation is high. Since the surface is believed to enhance [16,17] smectic ordering, the melting is more likely to take place in the middle of the cell. This process has been observed to occur when two sides of a cell containing Sm-A material are sheared with respect to each other [17].

To study this intermediate state we add to Eq. (1) the bulk smectic free energy contribution $f_s^{(b)}$:

$$f_s^{(b)} = -\alpha t|\psi|^2 + \frac{\beta|\psi|^4}{2} = -\alpha t \eta^2 + \frac{\beta \eta^4}{2} . \tag{16}$$

Here $t = (-T + T_{NA})/T_{NA}$ and α, β denote material constants. The minimum bulk smectic contribution corresponds to $\eta = \eta_b = \sqrt{\alpha t/\beta}$, yielding $f_s^{(b)} = -(\alpha t)^2/(2\beta)$.

We simplify the problem by setting $\gamma \equiv \gamma_{\parallel} = \gamma_{\perp}$ and $K \equiv K_{33} = K_{11}$ and assume a strong anchoring condition. The total free energy per unit surface F, already minimized through $\partial u/\partial x$, is then

$$\begin{aligned} F &= \int_{-L/2}^{L/2} f(x,\eta)dx \\ &= \int_{-L/2}^{L/2} \left[\frac{K}{2} \left(\frac{\partial \theta}{\partial x} \right)^2 + f_s^{(b)} + \gamma \eta^2 q_0^2 (1 - \epsilon - \cos\theta)^2 \right. \\ &\quad \left. + \gamma \left(\frac{d\eta}{dx} \right)^2 \right] dx . \end{aligned} \tag{17}$$

We assume that the intermediate state of the tilted–chevron-structure transition consists of the melted (nematic) region in the center of the cell extending over the size 2ξ. The distance over which the smectic order parameter is recovered is of the order of the smectic coherence length [9] $\xi=\sqrt{\gamma/(\alpha t)}=(1/\eta_b)\sqrt{\gamma/\beta}$. The remaining part of the cell is set to be in the bookshelf configuration with $\eta=\eta_b$. Finally we approximate the last term in Eq. (17) by $\int(d\eta/dx)^2dx\approx 2\xi(\eta_b/\xi)^2$. The corresponding approximate expression for the free energy $F_{\rm melt}$ per unit surface of the melted structure is

$$F_{\rm melt}\approx[r_s^{(b)}(\eta_b)+\gamma q_0^2\eta_b^2\epsilon^2](L-2\xi)+2\gamma\xi\left[\frac{\eta_b}{\xi}\right]^2$$
$$=Lf_s^{(b)}(\eta_b)$$
$$+\gamma q_0^2\eta_b^2 L\left[\epsilon^2\left[1\frac{2\xi}{L}\right]+\frac{3}{q_0^2L^2}\frac{L}{\xi}\right]. \quad (18)$$

We are going to compare $F_{\rm melt}$ relatively to the free energy per unit surface $F_{\rm chev}$ of the chevron structure. To estimate $F_{\rm chev}$ we assume (i) a well-developed chevron structure, (ii) that θ recovers linearly from $\theta=0$ at the bonding plates and in the middle of the cell to its saturated value $\theta\approx\sqrt{2\epsilon}$ on the scale described by the smectic penetration depth $\lambda=(1/\eta)\sqrt{K/(\gamma q_0^2)}$, and (iii) that $\eta\approx\eta_b$ in the whole cell. With this in mind we obtain

$$F_{\rm chev}\approx\int_{-L/2}^{L/2}\left[f(\eta_b)+\frac{K}{2}\left[\frac{\partial\theta}{\partial x}\right]^2\right]$$
$$\approx Lf_s^{(b)}(\eta_b)+\frac{4K\epsilon}{\lambda}$$
$$=Lf_s^{(b)}(\eta_b)+\gamma q_0^2\eta_b^2 L\left[4\epsilon\frac{\lambda}{L}\right]. \quad (19)$$

We define

$$B=\frac{F_{\rm melt}-Lf_s^{(b)}(\eta_b)}{F_{\rm chev}-Lf_s^{(b)}(\eta_b)}$$
$$=\frac{\epsilon^2(1-2\xi/L)+(3/q_0^2L^2)(L/\xi)}{4\epsilon\lambda/L} \quad (20)$$

as a measure of the energy barrier between the tilted and chevron structures.

We further assume the $\lambda=(1/\eta_b)\sqrt{K/(\gamma q_0^2)}$ and $\xi=(1/\eta_b)\sqrt{\gamma/\beta}$ values to be the same. Defining dimensionless quantities $y=L/\xi=L/\lambda$, $\delta=1/(q_0^2L^2)$, the expression for B can be rewritten as

$$B=\frac{\epsilon^2(y-2)+3\delta^2y^2}{4\epsilon}. \quad (21)$$

The barrier ratio $B(y)$ is plotted in Fig. 7. The value of y extends from $y=0$ at $T=T_{AN}$ to $y>10^4$ deep in the Sm-A phase. The chevron condition $\sigma=1$ translates to a condition that $y>4/\epsilon$, and we only plot $B(y)$ in this regime. The energy barrier is evidently relatively large compared to the chevron free energy, indicating that this process is unlikely to happen in practice.

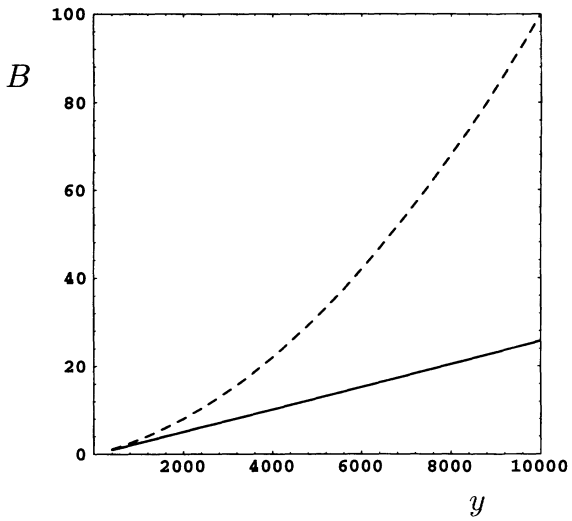

FIG. 7. Plot of $B(y)$ measuring the energy barrier for the chevron–tilted-structure transformation via melting of the tip of the chevron structure. In the calculations we set $d=3$ nm and $\epsilon=0.01$. Full line: $\delta=10^{-4}$ (corresponding to $L\approx 5$ μm); dotted line: $\delta=10^{-5}$ ($L\approx 50$ μm).

VII. SURFACE DISLOCATIONS

In this paper we have discussed the smectic structures induced in a thin layer caused by a mismatch between spatial periodicities favored by the surface and by the bulk. The mechanism for this mismatch is that the surface periodicity is in some sense frozen in, whereas the bulk periodicity is—at least weakly—temperature dependent.

Only in Sec V, and then not in detail, have we discussed the process whereby the surface periodicity can affect a bulk structure. In Sec. V we have introduced a surface potential W_p which favors a periodicity at the surface with wave number q_f. We have suggested that the smectic periodicity q in a cell will involve a compromise between surface and bulk tendencies.

In fact it seems likely that the equilibrium configuration can be more complicated still and involve domain structures which are inhomogeneous in the z direction as well as the x direction. Such structures, which will have some solitonlike properties, will be affected by bulk constraints in the center of the cell but surface constraints close to the walls. This will lead to localized layer bending and squashing close to the wall.

In the cases we consider $\epsilon=1-d_0/d_s>0$ and some strain can always be relieved by bending layers. However, if $\epsilon<0$ this is not a possibility and we can use this case to consider in principle general classes of surface configuration.

Depending on the strength of W_p it seems likely that at least three qualitatively different configurations exist.

(i) When positional anchoring is not present the layers adopt an undistorted bookshelf layer configuration. With increased W_p one possible way to release the imposed strain is by local layer rearrangement at the bounding plates. The resulting layer displacement field experiences

a solitonlike profile at $x \sim \pm L/2$ in the z direction enabling a partial satisfaction of the positional boundary condition.

(ii) When W_p is further increased the LC distortion at the surface progressively increases. At a critical value $W_p \sim W_p^{(1)}$ edge dislocations are incorporated into the layer structure. Dislocation axes, surrounded by a core of nematic liquid, are running along the y coordinate. The density of dislocations per unit length in the z direction is roughly $n(\epsilon) \sim \epsilon / d_0$.

(iii) At $W_p \sim W_p^{(2)} \geq W_p^{(1)}$ the surface potential is strong enough to unbind dislocations from the bounding plates towards the cell interior. In this strong positional anchoring regime the shift $\Delta x(W_p)$ of edge locations from the bonding plates depends on W_p. If $\Delta x(W_p) \sim L/2$ dislocations originating from different bounding plates might merge, forming again a dislocation-free bookshelf structure.

This general scenario is reminiscent of wetting, in which strong surface potentials induce a new surface phase [20]. The picture we have just outlined may also occur if $\epsilon > 0$, but now there are extra complications caused by the competition with layer tilt. We shall return to this problem in a future publication.

VIII. CONCLUSIONS

In this paper we have made a careful study of the way in which surface strain, or mismatch between the layer periodicities in the bulk and the surface, can induce chevron and tilted structures in smectic-A materials. Using the Landau–de Gennes free energy, we have shown that the formation and evolution of structures exhibits almost universal behavior as a function of a dimensionless parameter σ which we call the chevron number, where

$$\sigma = \frac{\epsilon \gamma_{\parallel} q_0^2 \eta^2 L^2}{2\pi^2 K_{11}} \left[1 + \epsilon \left[\frac{\gamma_{\parallel}}{\gamma_{\perp}} - 1 \right] \right] .$$

We have found threshold values σ_c and σ_t for the formation of the chevron structure and the tilted structure, respectively. Despite the experimental observation that chevron formation is more common than layer tilt, in general $\sigma_c > \sigma_t$.

Chevron and tilt formation is favored, evidently by high strain, but also by high smectic order parameter, high cell thickness, low nematic splay elastic constant, and proprinquity to the onset of the smectic-C phase. The underlying physical reason for chevron formation is that this is a mechanism to localize and hence reduce the strain caused by the layer mismatch.

The relative amplitude θ_i/θ_m behaves as $\theta_i/\theta_m \sim \sqrt{(\sigma - \sigma_i)/\sigma}$, where $i = \{c,t\}$ refers to the chevron and the tilted structure. The chevron number σ experiences drastic temperature variation near (i) the Sm-A–N second order transition where η tends to zero, (ii) the Sm-A–Sm-C transition where $\gamma_{\parallel}/\gamma_{\perp}$ diverges, and (iii) the Sm-A–Sm-B transition where K_{11} diverges. The threshold values σ_c, σ_t do not depend on K_{33} since the structures form via splay deformation. The bend elastic constant becomes important at later stages of the evolution.

For strong anchoring $\sigma_c = 1$ and $\sigma_t = \frac{1}{4}$. Weaker anchoring strength diminishes elastic distortions at the bounding plates. As a consequence the threshold values σ_t and σ_c decrease. In the limit $W_0 \to 0$ they tend to $\sigma_c = \frac{1}{4}$ and $\sigma_t = 0$.

Since the triggering parameter σ depends on η, the structures can even form discontinuously at a first order N–Sm-A phase transition. However, the necessary requirement for this is that at the phase transition the strain is already imposed and that $\sigma > \sigma_c$; this presupposes some sort of surface memory effect.

We have also made a qualitative analysis of hysteretic behavior associated with chevron formation and disappearance observed in recent experiments [5,6]. Our explanation is based (i) on the assumption that the smectic phase can establish a spatially periodic surface potential [16] and (ii) on the surface memory effect [15]. However, the clarification of the observed phenomena requires a more profound study.

The mechanism of the tilted structure formation is still unclear. Although its LC deformation is far lower than the chevron one, in practice the chevron structure is observed if it can exist. This indicates that it is kinematically difficult to reach the tilted structure. We suggest that formation of the tilted structure would require sliding of the established surface positional potential. This is either extremely slow or energetically costly so that the chevron structure is formed instead. In order to estimate the upper limit of the energy barrier separating the chevron and tilted structures we have considered the case when the transition between them is realized via melting at the chevron tip.

There are also other ways through which LC's can at least partly relax the mismatch between the surface potential anchoring and the spatial periodicity favored by a Sm-A phase. We have discussed the case where the strain imposed is relieved by forming domainlike structures. The qualitative appearance of these structures depends on the strength of the surface positional potential. In contrast to the chevron and tilted configurations, the domainlike structures are also possible for $\epsilon < 0$. These phenomena, which bear some resemblance to the statistical mechanics of wetting, require extensive further analysis.

There are many other systems which relax imposed strain in a chevronlike way. In our paper we have emphasized the similarity with Freedericksz transitions in nematic liquid crystals [9]. Limat and Prost [7] pointed out the analogy to Helfrich deformation in a Sm-A film. This problem has been recently studied in detail by Singer [21], who has observed that such phenomena are characteristic of all two dimensional systems whose inherent one dimensional order parameter spatial variation is perturbed.

In the future we shall extend this study to consider chevron formation in Sm-C materials. This case, although in principle similar to the case considered in this paper, presents considerable technical difficulties resulting from the increased number of relevant variables. This

case, however, is of considerable interest in view of its significance in the context of ferroelectric liquid crystal display device construction.

ACKNOWLEDGMENTS

S.K. gratefully acknowledges the financial support of the Slovenian Ministry of Science and Technology and Open Society Fund of Slovenia. We thank J. Prost, F. M. Leslie, I. W. Stewart, M. J. Towler, and E. Velasco for useful conversations.

APPENDIX: THE LIMAT-PROST MODEL

In this Appendix we briefly describe the relationship between our free energy formulation Eq. (3) and the formulation used by Limat and Prost [7]. Assuming strong anchoring boundary condition the (scaled) local free energy density is

$$g = g_n(\rho) + g_s(\rho) , \tag{A1}$$

where

$$g_n(\rho) = \frac{1}{2}\left[\frac{\partial\theta}{\partial\rho}\right]^2 (\cos^2\theta + a_3\sin^2\theta) , \tag{A2}$$

$$g_s(\rho) = \frac{L^2}{\lambda^2}\{a(w\cos\theta - \sin\theta)^2(1-\epsilon)^2 + [(1-\epsilon)(w\sin\theta + \cos\theta) - 1]^2\} . \tag{A3}$$

We first consider the nematic contribution $g_n(\rho)$. If θ is assumed small

$$\cos^2\theta + a_3\sin^2\theta \sim 1 + (a_3 - 1)\theta^2 \tag{A4}$$

and hence to leading order in θ the nematic contribution to the free energy is simply given by

$$g_n(\rho) = \frac{1}{2}\left[\frac{\partial\theta}{\partial\rho}\right]^2 . \tag{A5}$$

This term favors a uniform director.

The smectic contribution consists of two parts, the first of which is proportional to $a = \gamma_\perp/\gamma_\parallel$ and is concerned with local departures of the director from the layer normal. We simply ignore this by supposing that these departures are not present and $w = \tan\theta$ everywhere. Technically, however, this involves taking the limit $a \to \infty$, and it is not clear how the formal product of a large elastic constant and small consequent fluctuations will work out. We are left with the second part, which comes from departures of the layer thickness from its equilibrium value. We substitute $w = \tan\theta$ to obtain

$$g_s(\rho) = \frac{L^2}{\lambda^2}\left[(1-\epsilon)\left[\frac{\sin^2\theta}{\cos\theta} + \cos\theta\right] - 1\right]^2 = \frac{L^2}{\lambda^2}\left[\frac{1-\epsilon}{\cos\theta} - 1\right]^2 . \tag{A6}$$

In the limit of small θ

$$(\cos\theta)^{-1} \sim 1 + \frac{\theta^2}{2} , \tag{A7}$$

and hence Eq. (A7) reduces to

$$g_s(\rho) = \frac{L^2}{\lambda^2}\left[\frac{\theta^2}{2} - \epsilon\right]^2 . \tag{A8}$$

Combining Eqs. (A5) and (A8) we obtain

$$g(\rho) = \frac{1}{2}\left[\frac{\partial\theta}{\partial\rho}\right]^2 + \frac{L^2}{\lambda^2}\left[\epsilon - \frac{\theta^2}{2}\right]^2 , \tag{A9}$$

which is the free energy used by Limat and Prost.

[1] T. P. Rieker, N. A. Clark, G. S. Smith, D. S. Parmar, E. B. Sirota, and C. R. Safinya, Phys. Rev. Lett. **59**, 2658 (1987).
[2] Y. Ouchi, J. Lee, H. Takezoe, and A. Fukuda, Jpn. J. Appl. Phys. Lett. **27**, 725 (1988).
[3] M. Nakagawa, Displays **4**, 67 (1990).
[4] A. Meyere, H. Pauwels, and E. Ley, Liq. Cryst. **14**, 1269 (1993), and references therein.
[5] Y. Takanishi, Y. Ouchi, H. Takezoe, and A. Fukuda, Jpn. J. Appl. Phys. **28**, L487 (1989).
[6] Y. Ouchi, Y. Takanishi, H. Takezoe, and A. Fukuda, Jpn. J. Appl. Phys. **28**, 2547 (1989).
[7] L. Limat and J. Prost, Liq. Cryst. **13**, 101 (1993).
[8] P. G. de Gennes, Solid State Commun. **10**, 753 (1972).
[9] G. Vertogen and W. H. de Jeu, *Thermotropic Liquid Crystals* (Springer-Verlag, Berlin, 1988).
[10] T. C. Lubensky and S. R. Renn, Phys. Rev. A **41**, 4392 (1990).
[11] S. Kralj and T. J. Sluckin (unpublished).
[12] P. G. de Gennes, *The Physics of Liquid Crystals* (Oxford University, London, 1974).
[13] M. Kléman, J. Phys. (Paris) **35**, 595 (1974).
[14] W. H. Press, B. P. Flannery, S. A. Teukolsky, and W. T. Vetterling, *Numerical Recipes* (Cambridge University Press, Cambridge, 1986).
[15] N. A. Clark, Phys. Rev. Lett. **55**, 292 (1985).
[16] G. Durand, Liq. Cryst. **14**, 159 (1993).
[17] M. Cagnon and G. Durand, Phys. Rev. Lett. **70**, 2742 (1993).
[18] J. Chen and T. C. Lubensky, Phys. Rev. A **14**, 1202 (1976).
[19] R. Holyst, D. J. Tweet, and L. B. Sorensen, Phys. Rev. Lett. **65**, 2153 (1990).
[20] M. M. Telo da Gama and D. E. Sullivan, *Liquids and Interfaces* (Wiley, New York, 1986), p. 1.
[21] S. J. Singer, Phys. Rev. E **48**, 2796 (1993).